# Observer-based nonlinear Compensation of Friction in a Positioning System

Hermann Henrichfreise and Christian Witte

Cologne Laboratory of Mechatronics
University of applied sciences Cologne
Betzdorfer Str. 2, D-50679 Cologne, Germany

## Abstract

*Friction is an undesired phenomenon in many drive systems. Feedforward of a suitable estimate of friction is an effective method to compensate the friction-dependent position errors in the steady state. The speed of reconstruction of the real friction is crucial for the grade of improvements which can be achieved for the transient behaviour. A nonlinear model-based approach is presented in this paper which due to the reconstruction of the sign changes of friction yields good results. Moreover, the described control and compensation is easy to implement and turns out to be very robust in real operation.*

## 1. Introduction

Increasing demands for speed and accuracy of position control systems, for example in the fields of machine tools and robotics, require to abandon the still commonly used conventional control approaches and to apply up-to-date methods from optimal state space control. Its theoretical basis was laid already decades ago. With integrated tools for control design and realization, the implementation of state space control systems is no longer a tedious matter [1]. State space control allows active damping of elastic modes present in nearly every mechanism which results in a high control bandwidth. Additionally, external and internal disturbances can be compensated if the plant model is appropriately augmented for control design [2; 3; 4]. In reality, however, hard nonlinearities in the plant often deteriorate the good system behaviour attainable for the purely linear case. Suitable countermeasures are nonlinear extensions of the controller which recover the linear control system behaviour by compensating the nonlinear plant properties as much as possible. In this paper such a hard nonlinearity is given by friction in a compliant positioning system. Starting with a linear model-based compensation, different nonlinear model-based approaches for the estimation and compensation of friction are presented. Their relevance for high-speed and precise position control is shown with simulation and experimental results.

## 2. Plant and control

Figure 1 shows the structure of the electromechanical positioning system (EMPS) which is used at the CLM for experimental investigation of position control schemes for compliant systems with friction.

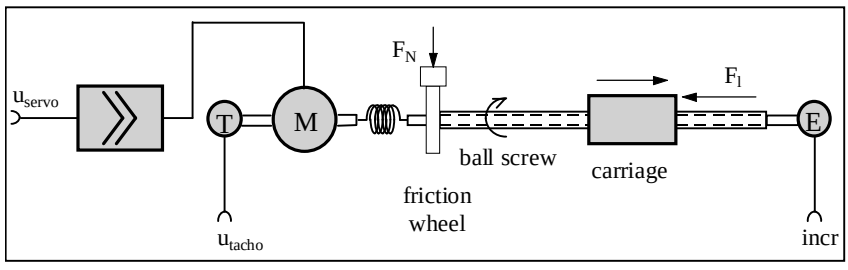


**Figure 1:** Electromechanical positioning system (EMPS).

The EMPS consists of a current-controlled DC-motor and a linear positioning unit. A backlash-free

ballscrew drive converts the rotary motion of the screw into the linear carriage displacement. Measurements used for control are the output voltage $u_{tacho}$ of a DC tacho generator at the drive side and the counter value incr of an incrementel encoder at the load side with a resolution equivalent to 1.25 µm carriage displacement. The control signal is the input voltage $u_{servo}$ for the motor reference current. A compliant coupling between motor and positioning unit whose stiffness and damping are only approximately known produces a mechanical resonance at about 100 Hz. Another shortcoming in the system is friction which is dominant in the ballscrew drive and results from its preloading for avoidance of backlash. In order to investigate the performance of compensation schemes with varying friction conditions, this load-side friction can be increased by a friction wheel. Figure 2 shows the measurement of friction torque versus carriage velocity valid in the context of this paper with dominant Coulombic and viscous friction.

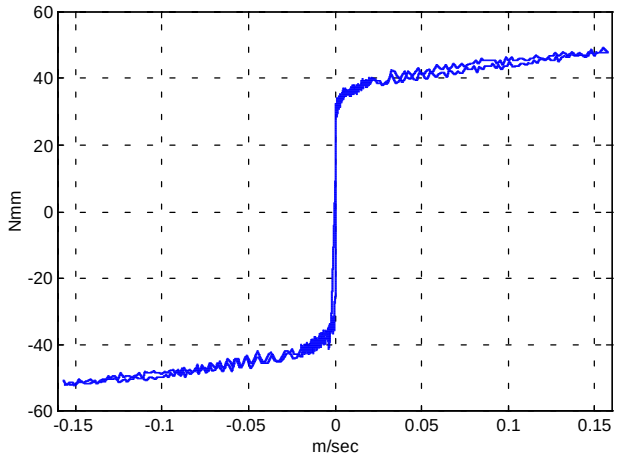


**Figure 2:** Friction torque versus carriage velocity.

The maximum absolute friction torque equals to about 30% of the available absolute motor torque of 0.1575 Nm. Without compensation in the position controlled system this friction causes a considerable error for the carriage position. Another reason for errors is the external disturbance force $F_l$ acting at the carriage.

With its structure and the described properties, the EMPS is typical for many drive systems in industrial applications.

The nonlinear plant model for simulation and a linearized model for control design are given in [5]. The motor torque, the drive-side (motor) and the load-side (ballscrew) angular positions and velocities are chosen as state variables. A linear time-invariant dynamic state space controller designed following the LQG/LTR-approach [6; 7; 8] is used for position control. Due to active vibration damping, this approach yields a high control bandwidth. It also shows a high robustness against uncertain plant properties. The minimum controller contains a complete feedback of the plant states and a feedforward of reference variables for the carriage motion. For friction compensation it will be augmented by a feedforward of an estimate for the disturbing load-side friction torque. The reference variables are the reference position, velocity, and acceleration for the carriage motion. They are provided by a reference profile generator. Figure 3 shows the top level structure of the position control system with the vector of the plant measurement outputs $\underline{y}_{pm}$ and the vector $\underline{y}_r$ containing the reference variables.

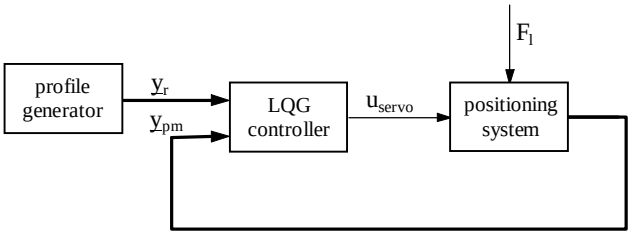


**Figure 3:** Structure of the positioning control system.

A systematic approach to control design and realization with development tools available on the market is described in [5].

## 3. System behaviour with different approaches for friction compensation

Basing on the minimum controller with plant state feedback and reference feedforward, different linear and nonlinear extensions for compensation of friction and their potentials of improvement will be presented by simulation and experimental results. The performance of the resulting control systems can be assessed by their reference and disturbance behaviour. Figures 4 and 5 show the time histories of the reference variables in the vector $\underline{y}_r$ which serve to investigate the reference behaviour. Both sets of signals make full use of the servo amplifier ranges. While the first set represents uni-directional reference motion of the carriage, the second contains a motion reversal which, due to the sign change of friction with the sign change of velocity, is more demanding for precise position control.

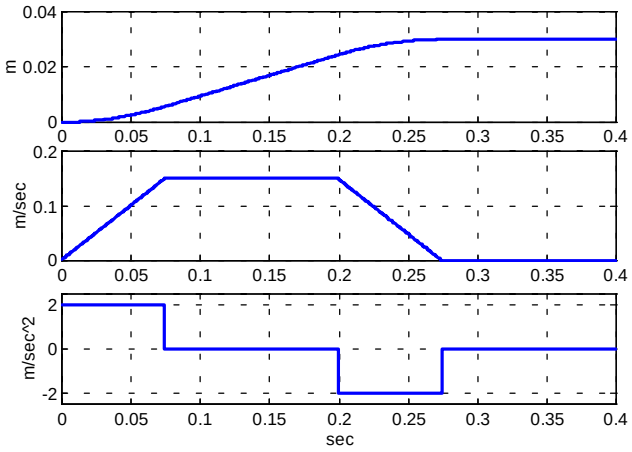


**Figure 4:** Uni-directional reference motion.

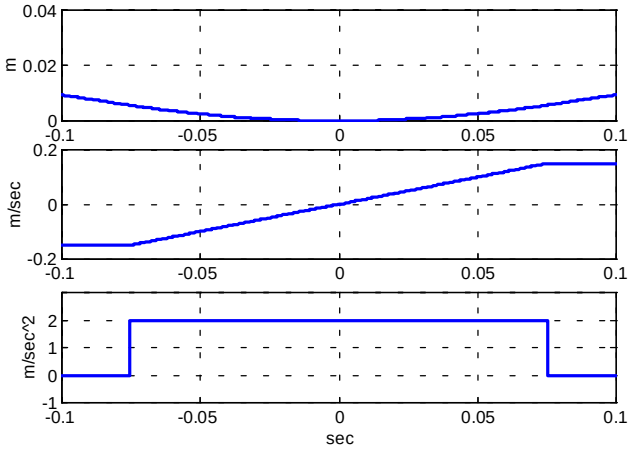


**Figure 5:** Reference motion with reversal.

In the following figures showing position error plots for reference excitation, the upper plot frame refers to the uni-directional reference motion and the lower frame to the reference motion with reversal.

The disturbance behaviour of the control system is assessed in simulation by applying a step of 150 N at t = 0.01 sec to the disturbance force input $F_l$.

To get an idea about the absolute improvements which will be achieved by friction compensation we are interested in the reference and disturbance behaviour of the system with the minimum controller without any measures against friction. Its structure with a linear observer to estimate the state vector of the plant, the matrix $\underline{K}_p$ for the state feedback, and the matrix $\underline{K}_r$ for feedforward of the reference variables in the vector $\underline{y}_r$ is illustrated in figure 6.

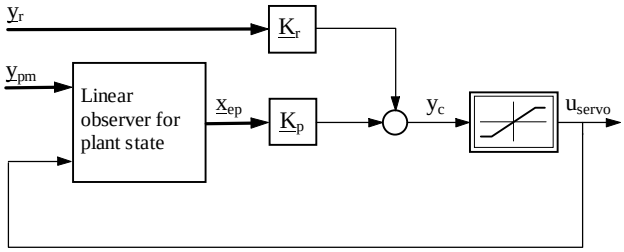


**Figure 6:** Controller without friction compensation.

With this controller, the reference behaviour of the position control system is given by the position error plots in figure 7. Figure 8 shows the position error for the disturbance step excitation at the input $F_l$ .

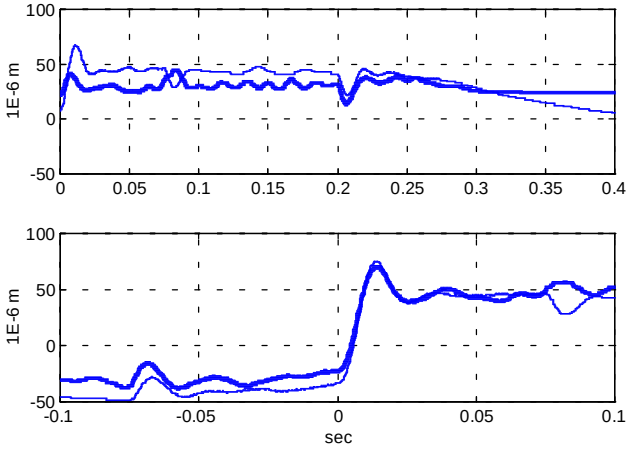


**Figure 7:** Measured (bold lines) and simulated position errors for reference excitation with controller of figure 6.

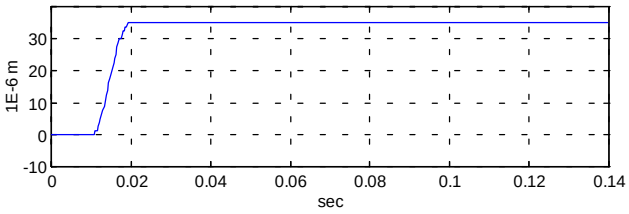


**Figure 8:** Simulated position error for disturbance step excitation with controller of figure 6.

These results are not very satisfactory. For position control to be accurate in the steady state, a compensation of friction is indispensable. The compensation schemes presented in the following chapters are those investigated in [9] which yielded the best results for for the EMPS control.

## 3.1 Linear model-based friction compensation

For linear control design with a linearized plant model, Coulombic friction can well be approximated by a constant disturbance input and hence be modelled by augmenting the plant with a linear integrator disturbance model with suitable initial condition [10; 11]. LQE design with this augmented plant model yields a linear observer for the augmented state vector (state vectors of plant and disturbance model), and LQR design the regulator gains for plant state feedback and disturbance state feedforward required for steady-state compensation of the non-measurable friction. For details of this control design specifically for the EMPS, the reader may refer to [5]. Figure 9 shows the resulting controller with observer for the state vector of the augmented plant and feedforward of the estimated disturbance state $x_{ed}$ to the control signal by the gain $K_d$.

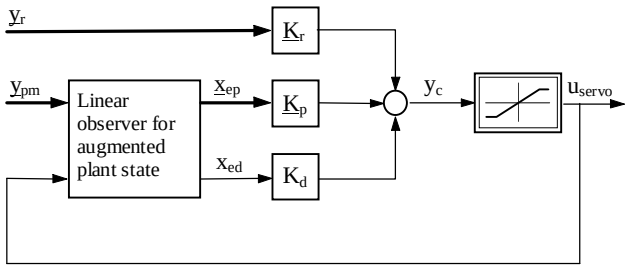


**Figure 9:** Controller with linear model-based disturbance estimation and feedforward.

In the position control for the EMPS shown in figure 3, this disturbance compensation is not only effective for friction, but also for step-shaped disturbance forces $F_l$. The results for reference and disturbance excitation are shown in figure 10 and 11. Compared to the results obtained without friction compensation (figures 7 and 8) or with conventional approaches to position control, the control shows a very good reference and disturbance behaviour. It is accurate in the steady state, transient position errors with start of motion from standstill, with motion reversals, and disturbance excitation, all accociated with step-shaped changes of friction, are rapidly compensated. The control turned out to be robust in every respect, especially against uncertain plant properties like inertias, stiffnesses and friction characteristics which are usually not exactly known in a real system.

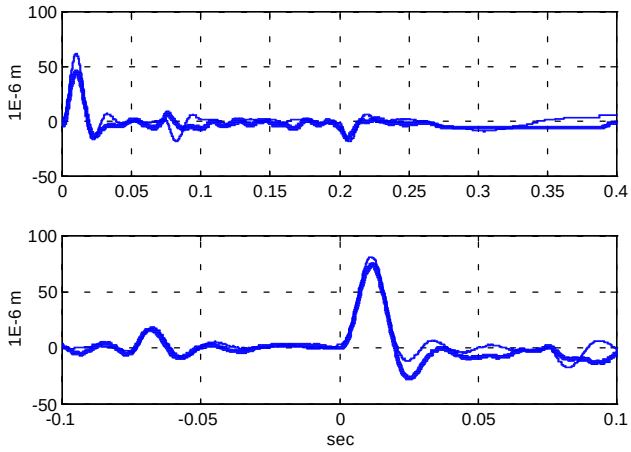


**Figure 10:** Measured (bold lines) and simulated position errors for reference excitation with controller of figure 9.

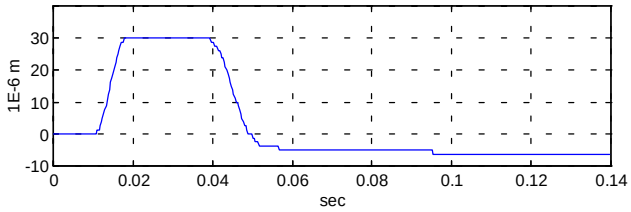


**Figure 11:** Simulated position error after disturbance step excitation with controller of figure 9.

In the disturbance step response shown in figure 11, the control seems to leave a steady-state position error. This error results from overshoot and sticking of the carriage in the static friction and is only slowly compensated, because the friction estimate $x_{ed}$ is delayed due to the limited observer bandwidth. This delay also influences the reference behaviour of the control system. Figure 12 shows the time history of the friction estimate for the reference motion with reversal (figure 5).

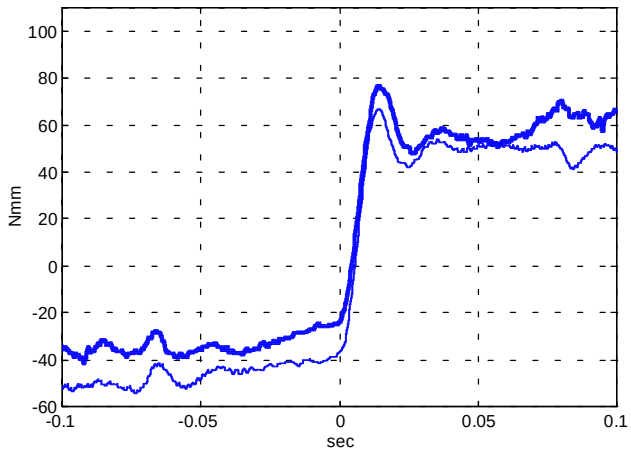


**Figure 12:** Measured (bold line) and simulated friction torque estimate $x_{ed}$ with motion reversal.

A faster reconstruction of the sign change of friction at t = 0 sec would be desirable to reduce the peak value and fall time of the corresponding transient position error in figure 10. In [4], the speed of friction estimation is increased by using the observation residual (the difference between the real and the estimated measuremet vector). For the present application the following nonlinear extension of the controller in figure 9, however, showed considerably better results [9].

The measured and simulated friction torque estimates from figure 12 differ by an offset of about 15 Nmm. This results from offset voltages in the power amplifier and inertias in the plant model used for observer design which do not exactly match the real plant properties [4].

## 3.2 Nonlinear model-based friction compensation

An obvious way to improve the estimation of friction, which can be found in other publications on friction compensation [12; 13], is to use a more realistic nonlinear friction model. We like to combine this approach with the linear model-based compensation from the previous chapter. A simple nonlinear model for friction is sufficient to reconstruct the step-shaped transition of friction at velocity zero. The remaining relatively slow change of friction with velocity is already well estimated with the linear model-based approach. Figure 13 shows the controller structure which is suggested in this paper.

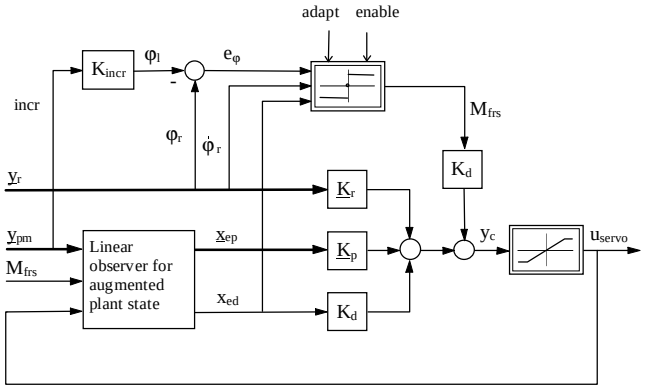


**Figure 13:** Controller with nonlinear model-based disturbance estimation and feedforward.

The output $M_{frs}$ of the nonlinear friction model is used to compensate the static friction torque in the positioning system when it starts moving or at motion reversals. If a positive or negative reference velocity $\dot{\varphi}_r$ is commanded to the controller, $M_{frs}$ will be set to the respective positive or negative maximum static friction torque (break-away torque) $M_{S+}$ or $M_{S-}$. With reference velocity zero, the friction model output depends on the position error $e_\varphi$. For a positive or negative error or an error equal to zero (which is defined in the range of the position measurement resolution around zero), $M_{frs}$ takes the respective values $M_{S+}$ , $M_{S-}$, or zero. Feedforward of this simple model for nonlinear friction to the control signal is done by the same gain $K_d$ which is used for the linear estimate. In order to avoid undesirable switching of the nonlinear friction estimate, the reference velocity is used as input into the friction model instead of the noisy velocity estimate from the observer. This simplification is possible due to the active vibration damping and high control bandwidth achieved by LQR control, and due to to the reference feedforward which let the load-side plant states closely follow the reference signals.

The above compensation of friction by the nonlinear model output relieves the linear compensation part. Only the difference between the actual friction in the plant and the nonlinear friction model output ist left for the estimate $x_{ed}$. To operate properly the linear observer for the augmented plant needs the injection of the nonlinear friction model output at the same location where the friction acts at the real system. This is realized by the additional observer input $M_{frs}$. By this inclusion of the nonlinear friction model in the estimation of the augmented plant state vector the nonlinear friction compensation corresponds with the theory for the linear compensation from chapter 3.1. A short derivation of the observer equations can be found in the appendix.

Good estimates of the maximum static friction torques $M_{S+}$ und $M_{S-}$ are crucial to let the suggested compensation scheme operate properly. These parameters of the nonlinear friction model have to be adapted to the actual friction values which alter with operating conditions. The linear estimate $x_{ed}$ offered to serve for the following adaptation procedure and thus became a third input to the friction model. The adaption is active when the reference velocity $\dot{\varphi}_r$ is within a given sufficiently small range around zero and its absolute value is decreasing. During such a deceleration phase, a first order lag filter approximates the mean value of the input signal $x_{ed}$. As soon as $\dot{\varphi}_r$ reaches zero, $M_{S+}$ or $M_{S-}$ depending on the preceding direction of motion are updated by

adding the filter output, and the filter state is reset for the next adaptation step. This procedure gradually reduces the range of $x_{ed}$ until the maximum static friction torque estimates reach their steady-state values. Adaptation only during deceleration, which is controlled with the input *adapt*, makes sure that the observer and, consequently, $x_{ed}$ has settled to its steady state. Moreover, adaptation should only be performed during special (learning) phases without external disturbance excitations. This avoids that external forces are misinterpreted as friction which would result in undesirable overcompensation when the forces cease to act. The adaptation can be stopped and the friction model output set to zero by resetting the input *enable*. A more detailed description of the friction model is given in [9].

Figures 14 and 15 present the results obtained with the nonlinear friction compensation together with those from the purely linear approach from chapter 3.1.

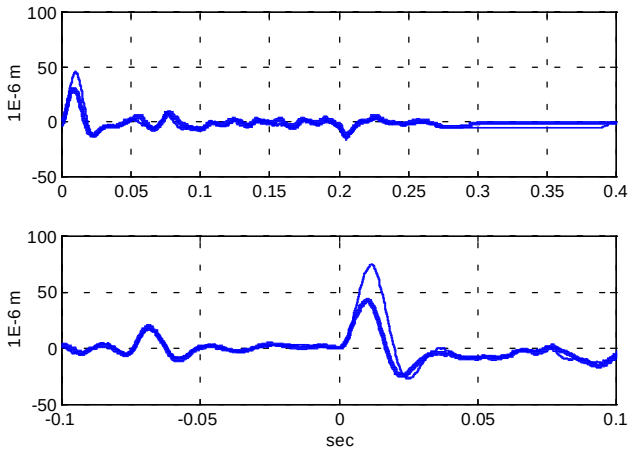


**Figure 14:** Measured position errors for reference excitation with controller of figure 13 (bold lines) and 9.

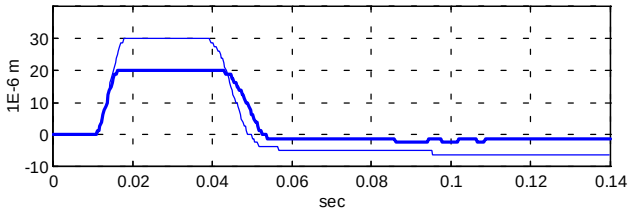


**Figure 15:** Simulated position error after disturbance step excitation with controller of figure 13 (bold line) and 9.

Because as in the previous chapters simulation and measurement results correspond well, and in order to avoid messy plots, the simulation results will not be shown in the following figures for the reference excitation and friction torque estimates.

Lower peak values and shorter fall times of the transient position errors become particularly clear for the motion reversal where the friction torque changes its sign. This results from the good reconstruction of friction by the nonlinear model in the controller. According to figure 16, the friction torque estimate is the sum of the nonlinear friction model output $M_{frs}$ (straight thin line) and the linear estimate $x_{ed}$ of the difference between real friction and friction model output (noisy thin line). Again offset voltages in the power amplifier and a plant model for observer design whose inertias do not exactly match with those of the real plant lead to an offset in the resulting friction torque estimate.

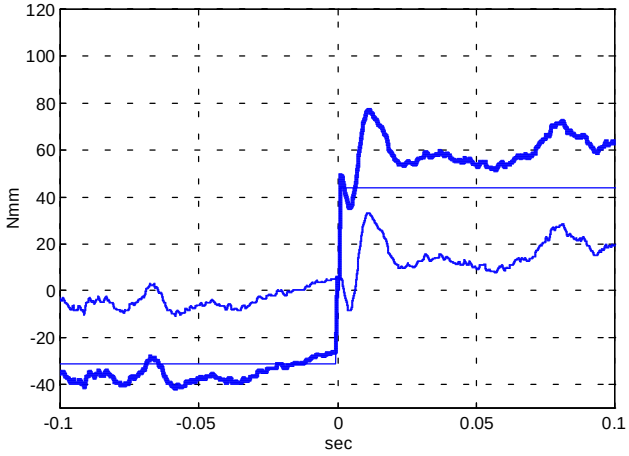


**Figure 16:** Measured friction torque estimates with controller of figure 13 and motion reversal.

As for the reference excitation, the position error for a disturbance step input (figure 15) shows a significantly smaller peak value. The error reaches the band of ±1.25 µm in a considerably shorter time.

The above improvements become even more significant with higher friction torques or reduced bandwidth of the linear observer, which may be imposed for cost reasons by mechanical components of lower quality or less performing real time hardware for controller realization. In figure 17 this is demonstrated for the case that the bandwidth of disturbance estimation in the augmented plant observer is reduced to 50% of its previous value. Due to the still good reconstruction of the friction torque (see figure 18), the influence on the position errors is only marginal with nonlinear friction compensation.

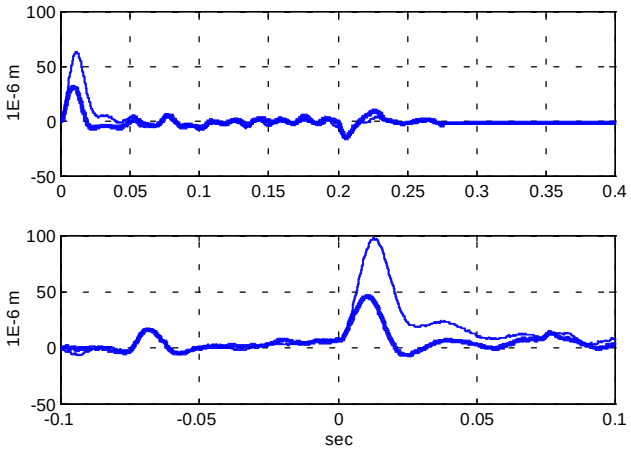


**Figure 17:** Measured position errors for reference excitation with controller of figure 13 (bold lines) and 9. Reduced bandwith of linear disturbance estimation.

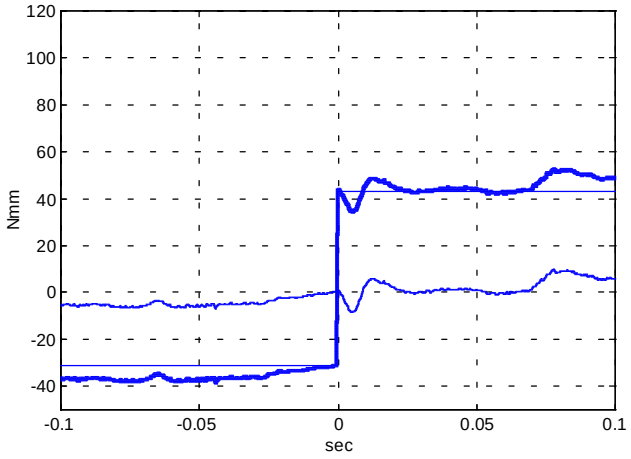


**Figure 18:** Measured friction torque estimates with controller of figure 13 and motion reversal. Reduced bandwidth of linear disturbance estimation.

Another approach for friction compensation with the nonlinear friction model described above is shown in figure 19. In this controller structure, the friction model is not included in the estimation of the augmented plant state vector. The linear observer of chapter 3.1 without additional input for injection of the nonlinear friction model output is used. Correspondingly, the friction model output is not fed back with the controller output to the observer control signal input, but only fed forward to the plant control input. The inverse of the power amplifier gain between reference current input and motor torque is used for the feedforward, which in a strict sense is only valid if the transfer function between the control signal (reference current) and disturbance input of friction in the plant were proportional. This would be the case for a rigid system and power electronics without time lag. The nonlinear friction model in the feedforward path effects a pre-compensation of friction for the uncontrolled plant.

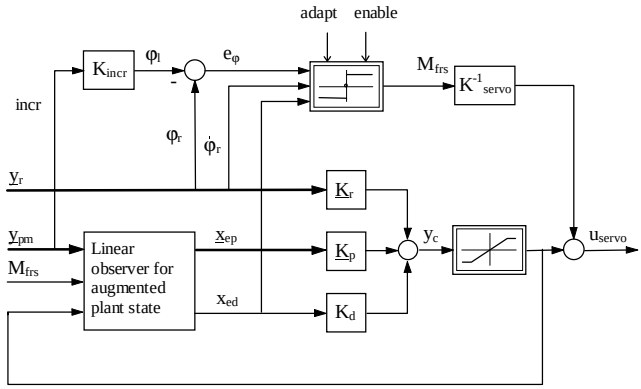


**Figure 19:** Controller with nonliner friction model in feedforward path.

The results with this approach are presented in figure 20 and 21. Compared with figure 14, the reference time responses show reduced error fall times but larger undershoot of the position errors. Both effects result from a larger overshoot in the friction torque estimates after step-shaped changes of friction in the plant, which becomes clear by comparing the results in figure 22 and figure 16.

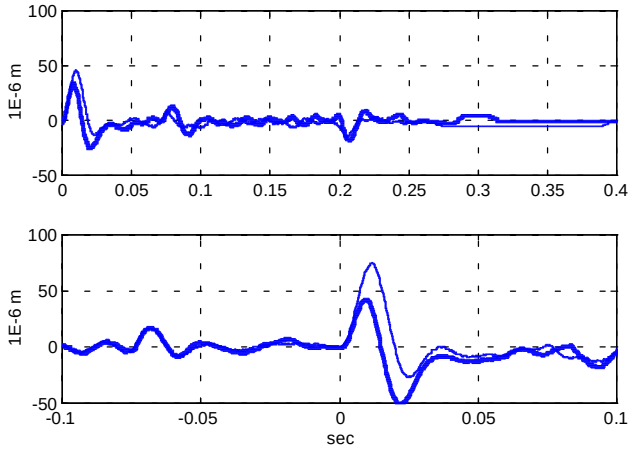


**Figure 20:** Measured position errors for reference excitation with controller of figure 19 (bold lines) and 9.

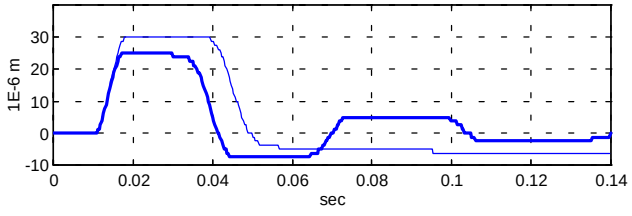


**Figure 21:** Simulated position error after disturbance step excitation with controller of figure 19 (bold line) and 9.

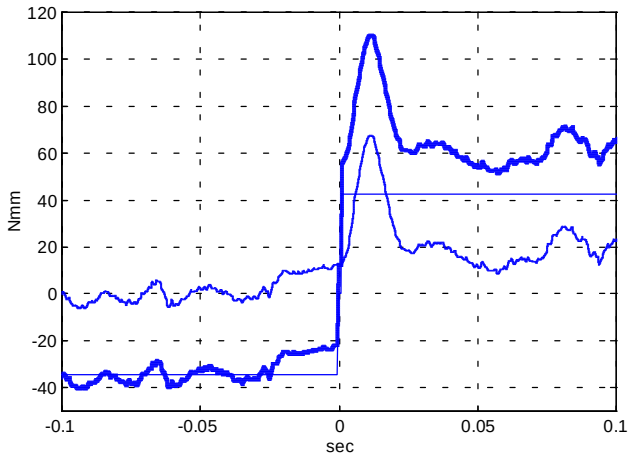


**Figure 22:** Measured friction torque estimates with controller of figure 19 and motion reversal.

While the controller of figure 13 is to be preferred for reference excitation, due to its smaller error settling times the controller of figure 19 could be taken into consideration for pure disturbance excitation. With the latter, the controlled system also appears slightly stiffer if the screw is manually twisted in the experiment. A combination of both structures could work as follows: If a reference motion is commanded to the system, the controller of figure 13 will be active. At standstills it will be replaced by the controller of figure 19 by switching the observer input and compensation path for the friction model output $M_{frs}$.

Simulation and experimental results revealed that the good robustness properties of the controller from chapter 3.1 are not affected when it is extended with the nonlinear friction model as described above.

## 3.3 Dynamic feedforward

In the previous chapters we used proportional feedforward to compensate internal and external disturbancies and the resulting position errors. However, since it does not regard the dynamics between the feedforward control and disturbance inputs of the system, this compensation is only effective in the steady state. As suggested in [4], the remaining potential for the transient behaviour can be used by a dynamic feedforward where the proportional gain is substituted by a transfer function. The inverse of the transfer function between the control and disturbance input is required to fully compensate the disturbance from the system response. Figure 23 shows the controller structure from the previuos chapter with the dynamic feedforward function $G_{cd}^{-1}(s)$, where $G_{cd}(s)$ is the transfer function between the control input and the load-side friction torque for the closed-loop system.

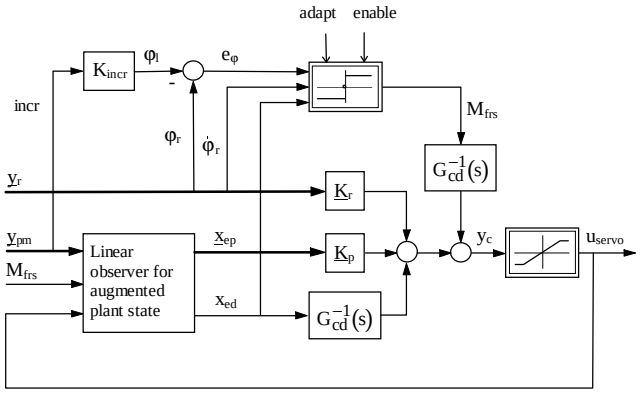


**Figure 23:** Controller with nonlinear model-based disturbance estimation and dynamic feedforward.

In [4] the implementation of this dynamic feedforward failed due its differentiating transfer characteristic and a noisy friction estimate which together resulted in an extensively noisy control signal. Since with the approach suggested in this paper the friction estimates are not much affected by noise, dynamic feedforward seemed to be implementable. In this case, however, the digital realization of $G_{cd}^{-1}(s)$ became a tedious job. Due to a limited processor performance its higher frequency dynamics could only be coarsely approximated. Additionally, for the reference excitation, the differentiating characteristic of $G_{cd}^{-1}(s)$ let the control signal exceed the power amplifier saturation bounds. No further improvement compared to the results presented in the previous chapter could thus be obtained.

# 4. Conclusions

Compensation of friction by feedforward of a suitable estimate for this non-measurable disturbance is a feasible method to reduce the position errors in the control of drives with friction. In this paper, a linear estimate was evaluated with a linear observer for the plant which was augmented by an appropriate disturbance model. In order to improve the linear estimate, an adaptive nonlinear friction model was introduced which provided the reconstruction of the sign change of friction in the plant. Results for two controller structures showed a considerable improvement of the position control. A compensator

which can switch between the two structures could combine their advantages both for reference and disturbance excitation.

Dynamic feedforward suggested in [4] seemed to be a promising improvement due to the good reconstruction of the friction in the plant. Problems to digitally implement the higher frequency dynamics of the feedforward and a control signal exceeding the actuator saturation bounds were the reasons to abandon this approach.

The presented friction compensation scheme is well suitable for numerous industrial applications. It turned out to be very robust and is easy to realize. Further work is planned to develop a module for local friction compensation on drive level [3] to be applied in coupled mechanisms with several drives like robots.

# Appendix

**Nonlinear observer for the augmented plant**

Given the state space equations of the linear plant model

$$\begin{aligned} \dot{\underline{x}}_p &= \underline{A}_p \underline{x}_p + \underline{B}_{pc} \underline{u}_{pc} + \underline{B}_{pd} \underline{u}_{pd} \\ \underline{y}_{pm} &= \underline{C}_{pm} \underline{x}_p + \underline{D}_{pmc} \underline{u}_{pc} + \underline{D}_{pmd} \underline{u}_{pd} \end{aligned} \qquad \text{(A1)}$$

with the state vector $\underline{x}_p$, the control input vector $\underline{u}_{pc}$, the disturbance input vector $\underline{u}_{pd}$, and the measurement output vector $\underline{y}_{pm}$ . In the special case of the EMPS, the disturbance input vector is a scalar variable, the sum $u_{pd} = M_{frl} + F_l / i$ of the load-side friction torque and the load torque acting on the screw, which is the quotient of the disturbance force and the ballscrew gear ratio. We further assume that the disturbance acting at the plant disturbance input can be sufficiently approximated by the disturbance model

$$\begin{aligned} \dot{\underline{x}}_d &= \underline{A}_d \underline{x}_d \,, \;\; \underline{x}_d(t=0) = \underline{x}_{d0} \\ \underline{y}_d &= \underline{C}_d \underline{x}_d + \underline{f}_d(.) \end{aligned} \qquad \text{(A2)}$$

as a sum of the output of a linear model with suitable initial condition and a nonlinear function $f_d(.)$ of control system variables. The respective terms for the EMPS are the outputs of a integrator disturbance model and the nonlinear friction model of chapter 3.2. The approximation $\underline{u}_{pd} \approx \underline{y}_d$ and putting (A2) in (A1) yield the augmented plant model

$$\begin{aligned} \dot{\underline{x}} &= \underline{A}\, \underline{x} + \underline{B}\, \underline{u}_{pc} + \underline{E}\, \underline{f}_d(.) \\ \underline{y}_{pm} &= \underline{C}\, \underline{x} + \underline{D}\, \underline{u}_{pc} + \underline{F}\, \underline{f}_d(.) \end{aligned} \qquad \text{(A3a)}$$

with the augmented state vector

$$\underline{x} = \begin{bmatrix} \underline{x}_p \\ \underline{x}_d \end{bmatrix} \qquad \text{(A3b)}$$

and the matrices

$$\underline{A} = \begin{bmatrix} \underline{A}_p & \underline{B}_{pd}\underline{C}_d \\ \underline{0} & \underline{A}_d \end{bmatrix}, \; \underline{B} = \begin{bmatrix} \underline{B}_{pc} \\ \underline{0} \end{bmatrix}, \; \underline{E} = \begin{bmatrix} \underline{B}_{pd} \\ \underline{0} \end{bmatrix} .$$
$$\underline{C} = \begin{bmatrix} \underline{C}_{pm} & \underline{D}_{pmd}\underline{C}_d \end{bmatrix}, \; \underline{D} = \underline{D}_{pmc} \,, \; \underline{F} = \underline{D}_{pmd} \qquad \text{(A3c)}$$

The nonlinear observer

$$\begin{aligned} \dot{\underline{x}}_e &= (\underline{A} - \underline{L}\underline{C})\, \underline{x}_e + (\underline{B} - \underline{L}\underline{D})\, \underline{u}_{pc} + \underline{L}\, \underline{y}_{pm} + (\underline{E} - \underline{L}\underline{F})\, \underline{f}_d(.) \\ &= \underline{A}_e \underline{x}_e + \underline{B}_e \underline{u}_e \\ \underline{y}_e &= \underline{x}_e \end{aligned} \qquad \text{(A4a)}$$

is used to estimate the augmented state vector with the state and the input vector

$$\underline{x}_e = \begin{bmatrix} \underline{x}_{ep} \\ \underline{x}_{ed} \end{bmatrix}, \; \underline{u}_e = \begin{bmatrix} \underline{u}_{pc} \\ \underline{y}_{pm} \\ \underline{f}_d(.) \end{bmatrix}, \qquad \text{(A4b)}$$

the matrices

$$\underline{A}_e = \underline{A} - \underline{L}\underline{C} \,, \; \underline{B}_e = \begin{bmatrix} \underline{B} - \underline{L}\underline{D} & \underline{L} & \underline{E} - \underline{L}\underline{F} \end{bmatrix} \qquad \text{(A4c)}$$

and the observer gain matrix $\underline{L}$. Corresponding with the block diagram in chapter 3.2, the value of the nonlinear function $\underline{f}_d(.)$ is interpreted as an external input to a linear observer subsystem. The observer gain matrix is designed with the linear model of the augmented plant given by equations (A3a) without the additional terms $\underline{E}\, \underline{f}_d(.)$ and $\underline{F}\, \underline{f}_d(.)$, which must be observable. The associated linear observer is used in the controller of chapter 3.1.

The output

$$\underline{y}_{ed} = \underline{C}_d \underline{x}_{ed} \qquad \text{(A5)}$$

of the linear disturbance model included in the observer represents an estimate of the difference between the the real disturbance acting on the plant and the nonlinear function $\underline{f}_d(.)$. For the EMPS, this output is identical with the state of the integrator disturbance model and is used in chapter 3.2 to adapt the nonlinear friction model to the actual friction in the plant.

## References


[1] *Hanselmann, H.:* DSP in Control: The Total Development Environment. International Conference on Signal Processing Applications & Technology ICSPAT'95, Boston, MA, USA, October 24-26, 1995.

[2] *Kasper, R.:* Entwicklung und Erprobung eines instrumentellen Verfahrens zum Entwurf von Mehrgrößenregelungen. Fortschritt-Berichte VDI, Reihe 8, Nr. 90, VDI-Verlag, Düsseldorf 1985.

[3] *Henrichfreise, H.:* Aktive Schwingungsdämpfung an einem elastischen Knickarmroboter. Fortschritte der Robotik, Band 1, Vieweg-Verlag, Braunschweig 1989.

[4] *Neumann, R.:* Beobachtergestützte dezentrale entkoppelnde Regelung von Robotern mit elastischen Gelenken. Fortschritt-Berichte VDI, Reihe 8, Nr. 529, VDI-Verlag, Düsseldorf 1996.

[5] *Henrichfreise, H.:* Prototyping of a LQG Compensator for a Compliant Positioning System with Friction. TRANSMECHATRONIK - Entwicklung und Transfer von Entwicklungssystemen der Mechatronik, HNI-Verlagsschriftenreihe, Volume 23, 1. Edition, Editor: Jürgen Gausemeier, Paderborn 1997.

[6] *Doyle, J. C., and Stein, G.:* Robustness with Observers. IEEE Trans. on Automatic Control, Vol. AC-24, p. 607-611, 1979.

[7] *Friedland, B.:* Control System Design. McGraw-Hill, 1986.

[8] *Lewis, F. L.:* Applied Optimal Control and Estimation. Prentice Hall, Englewood Cliffs, NJ, USA, 1992.

[9] *Henrichfreise, H., and Witte, C.:* Experimental Comparison of Observer-Based Friction Compensation Schemes for an Electromechanical Positioning System. Paper at the CLM, FB KT, Polytechnic Cologne 1997.

[10] *Friedland, B., Hutton, F. M., Williams, C., and Ljung, B.:* Design of Servo for Gyro Test Table using Linear Optimum Control Theory. IEEE Trans. on Automatic Control, p. 293-296, April 1976.

[11] *Ackermann, J., and Müller, P. C.:* Dynamical behaviour of nonlinear multibody system due to Coulomb friction and backlash. Preprints of IFAC/IFIP/IMACS International Symposium on Theory of Robots, p. 289-295, Wien 1986.

[12] *Canudas de Wit, C., Olsson, H., Aström, K.J., and Lischinski P.:* A new model for control of systems with friction. IEEE Trans. on Automatic Control, Vol. 40, No. 3, p. 419-425, March 1995.

[13] *Amin, J., Friedland, B., and Harnoy, A.:* Implementation of a friction estimation and compensation technique. IEEE Control Systems Magazine, August 1997.